Communication: Structural locking mediated by a water wire: A high-resolution rotational spectroscopy study on hydrated forms of a chiral biphenyl derivative

Sérgio R. Domingos, Cristóbal Pérez, and Melanie Schnell

Articles you may be interested in

Communication: Structural locking mediated by a water wire: A high-resolution rotational spectroscopy study on hydrated forms of a chiral biphenyl derivative

Sérgio R. Domingos,[1,2,3] Cristóbal Pérez,[1,2,3] and Melanie Schnell[1,2,3,a)]

[1]*Max Planck Institute for the Structure and Dynamics of Matter, Luruper Chaussee 149, 22761 Hamburg, Germany*
[2]*Center for Free-Electron Laser Science, Luruper Chaussee 149, 22761 Hamburg, Germany*
[3]*The Hamburg Centre for Ultrafast Imaging, Universität Hamburg, Luruper Chaussee 149, 22761 Hamburg, Germany*

We report the observation of structural changes in an axially chiral molecule, biphenyl-2-carboxaldehyde, due to aggregation with water. Using high-resolution broadband rotational spectroscopy we find that two water molecules link opposite sides of the molecule, resembling a water wire. We show that this effect can be explained by a cooperative rearrangement of both molecule and a water dimer. Hydrogen bonding interactions are shown to change the original structure upon aggregation of water. This phenomenon is insightful on the role of microsolvation in assisting structural morphing of stereo-selective chiral molecular systems. *Published by AIP Publishing.* [http://dx.doi.org/10.1063/1.4966584]

Water mediates the dynamics of biological processes from protein folding[1] to proton transport in membranes.[2] Localised solvation is presumed to effectively alter the binding efficiency of organic ligands to biological receptors, determining the availability, rate, and specificity of the binding. Consequently, assisted docking of ligands to receptors via intermediate local interactions with water molecules has been extensively modelled.[3] The interplay between structure and function of a biochemical system is tentatively better described by considering interactions with naturally occurring aqueous environments. Yet, a full comprehensive picture of such interactions is not established.

Isolated micro-solvated molecules in the gas phase have become an appealing target to reveal the stepwise hydration of molecular systems.[4–12] For example, high-resolution spectroscopy was recently employed to investigate water-mediated interactions between amide linkages, revealing hydrogen bonding cooperativity effects that are key to protein folding dynamics.[13] Unraveling the intermolecular binding forces and their role mediating more complex processes supports our understanding of hydration of biological systems and consequently improves methods for drug design.[3] Chiral molecules with axial chirality such as biphenyl-type systems, i.e., systems where rotation about an axis changes the handedness of the molecule, are generally of interest due to their low interconversion barriers between energetically equivalent stereoisomers.

Structural studies combining supersonic expansions with high-resolution rotational spectroscopy[14] provide a powerful means to probe molecular complexes with a selected number of water molecules aggregated to the target system. With the implementation of short and intense microwave chirps in broadband excitation schemes, as in chirped-pulse Fourier-transform microwave (CP-FTMW) spectroscopy, it is possible to record rotational spectra of complex, flexible molecules spanning several GHz with a single acquisition.[15] Here we use CP-FTMW spectroscopy combined with the cold and isolated conditions of a supersonic jet and complemented with theoretical methods to reveal the structures of free and micro-solvated biphenyl-2-carboxaldehyde (BPCO). All measurements were performed using the Hamburg COMPACT spectrometer. A complete description of the experimental setup can be found in Ref. 16. Additional upgrades to this design have been reported elsewhere.[17,18] Further experimental details can be found in the supplementary material. The experiments are supported by quantum-chemical calculations using Gaussian09.[19] The initial guesses for the geometries of the BPCO-water clusters were obtained using the program ABCluster.[20] A list of valid candidates was then further optimised using Moller-Plesset perturbation theory (MP2) with the 6-311++G(d,p) basis set and density functional theory (B3LYP-D3) including Grimme's empirical dispersion correction and the aug-cc-pVTZ basis set.

Fig. 1 shows the calculated potential energy surface displaying the barrier separating the stereoisomers of BPCO. The two stereoisomers have calculated dihedral angles of $\phi = -52.7°$ (blue) and $\phi = -127.3°$ (red), respectively. In Fig. 2 we show the broadband microwave spectrum of BPCO. A total of 138 rotational transitions were assigned and the rotational constants were determined through a recurrent fit using the A-reduced rigid rotor Hamiltonian as implemented in PGOPHER.[21] Quartic centrifugal distortion constants were also well determined. A summary of the fitted spectroscopic parameters is shown in Table I. We find

a)Author to whom correspondence should be addressed. Electronic mail: melanie.schnell@mpsd.mpg.de
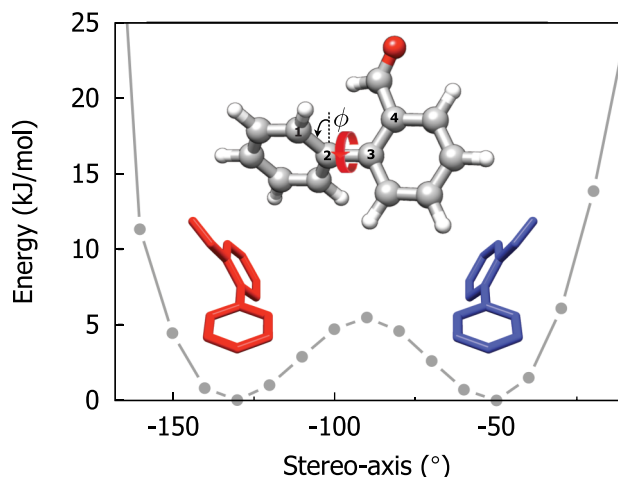
FIG. 1. Relaxed potential energy scan of the stereo-axis of BPCO, represented by the dihedral angle ϕ connecting the two phenyl moieties. The calculation was performed using density functional theory at the B3LYP-D3/aug-cc-pVTZ level of theory. The energy barrier separating the two stereoisomers is just above 5 kJ/mol (420 cm^{-1}). The dihedral coordinate established by the numbered atoms defines the chiral axis.
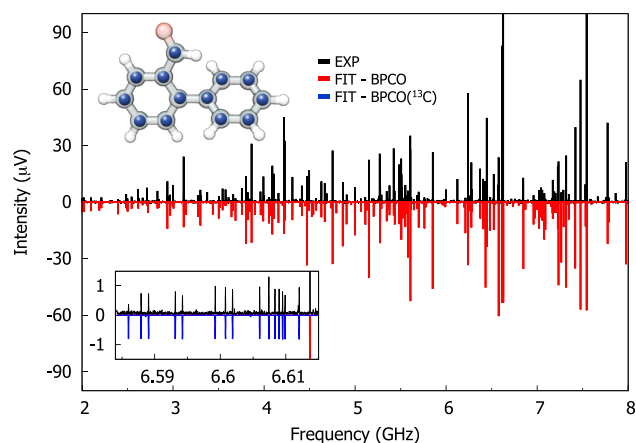

FIG. 2. Broadband rotational spectrum of BPCO from 2 to 8 GHz (1.9 M averages, 17 h of measurement time). The upper trace (in black) shows the experimental spectrum using neon as a carrier gas. The lower trace represents simulations obtained from the fitted spectroscopic parameters reported in Table I. Inset: portion of the spectrum highlighting the satellite transitions corresponding to the singly substituted ^{13}C isotopologues. The lower trace (in blue) represents the simulated spectrum. In the upper left we show an overlay of the experimental (see supplementary material) and the predicted (B3LYP-D3/aug-cc-pVTZ) structure of BPCO. The blue spheres represent the experimentally determined carbon atom positions.

no evidence for large amplitude motions for free BPCO. A signal-to-noise ratio (SNR) of 850:1 allowed us to observe all thirteen distinct spectra for the singly substituted ^{13}C isotopologues in natural abundance (see inset of Fig. 2). With these conditions we were able to employ the substitution, r_s, method to derive the positions of the carbon atoms in the principal axis frame using the Kraitchman equations.[22,23] This method provides a way to extract atom coordinates from the changes in the moments of inertia upon isotopic substitution. An overlay of the experimentally determined atom positions and a theoretical prediction at the B3LYP-D3/aug-cc-pVTZ level of theory is shown in Fig. 2 (upper left). The good agreement between experiment and theory regarding the twist angle (ϕ) of unbound BPCO, $-56.7(\pm4.2)°$ and

$-55.4°/-52.7°$ (MP2/DFT) (see Table I), respectively, gives us confidence in the reliability of our calculations for further comparisons.

In another set of experiments we prepared our molecular beam with a mixture of BPCO and water (2M averages, 18 h of measurement time). Fig. 3 shows two sections of the broadband spectrum highlighting fitted rotational transitions for three complexes of water with BPCO. Fitted rotational parameters are given in Table I for all observed species. In Fig. 4 we present the calculated molecular structures of BPCO-1w(I), BPCO-1w(II), and BPCO-2w(II), which are found to reproduce the experimental rotational constants.

TABLE I. Rotational constants, dipole moments, and centrifugal distortion constants for biphenyl-carboxaldehyde (BPCO) and water aggregates. The errors given here for the measured values are standard errors. N is the number of lines included in the fit and σ is the standard deviation of the fit. The values of ϕ are defined by the dihedral angle as depicted in Fig. 1.

	BPCO		BPCO-1w(I)		BPCO-1w(II)		BPCO-2w(II)	
	Exp	B3LYP^a/MP2^b	Exp	B3LYP^a/MP2^b	Exp	B3LYP^a/MP2^b	Exp	B3LYP^a/MP2^b
A/MHz	1234.899 70(25)	1238.95/1226.79	974.767 25(54)	978.94/968.36	627.436 61(55)	620.37/656.88	496.656 14(61)	502.18/506.83
B/MHz	501.695 03(15)	503.75/502.90	358.036 77(13)	364.09/362.20	498.725 77(28)	501.36/496.66	437.482 28(30)	440.21/430.91
C/MHz	386.795 24(13)	386.53/387.84	278.110 19(11)	281.28/280.41	296.548 10(27)	295.20/301.99	258.286 01(21)	257.80/260.46
D_J/kHz	0.010 4(11)	...	0.014 46(42)	...	0.012 9(16)	...	0.964 8(419)	...
D_{JK}/kHz	0.103 1(35)	...	0.012 8(54)	...	0.236(12)	...	−0.422(15)	...
D_K/kHz	−0.056 2(85)	...	0.272(30)	...	0.197(18)	...	0.526(30)	...
d_J/kHz	0.002 03(50)	...	0.002 97(23)	...	...	...	0.036 9(23)	...
d_K/kHz	0.068 5(91)	...	−0.051 0(84)	...	...	...	−0.097 2(86)	...
$|\mu_a|$/D	...	1.53/1.22	...	3.43/3.02	...	0.28/0.93	...	1.95/1.56
$|\mu_b|$/D	...	3.25/3.01	...	1.73/1.25	...	3.67/2.40	...	1.74/0.87
$|\mu_c|$/D	...	0.17/0.04	...	0.60/0.85	...	0.48/0.72	...	0.96/1.18
N	138	...	125	...	65	...	37	...
σ/kHz	4.5	...	5.4	...	8.7	...	2.8	...
ϕ/deg	−56.7 ± 4.2	−52.7/−55.4	...	−52.7/−55.3	...	−51.8/−53.3	...	−48.3/−50.6

^{a}aug-cc-pVTZ basis set.
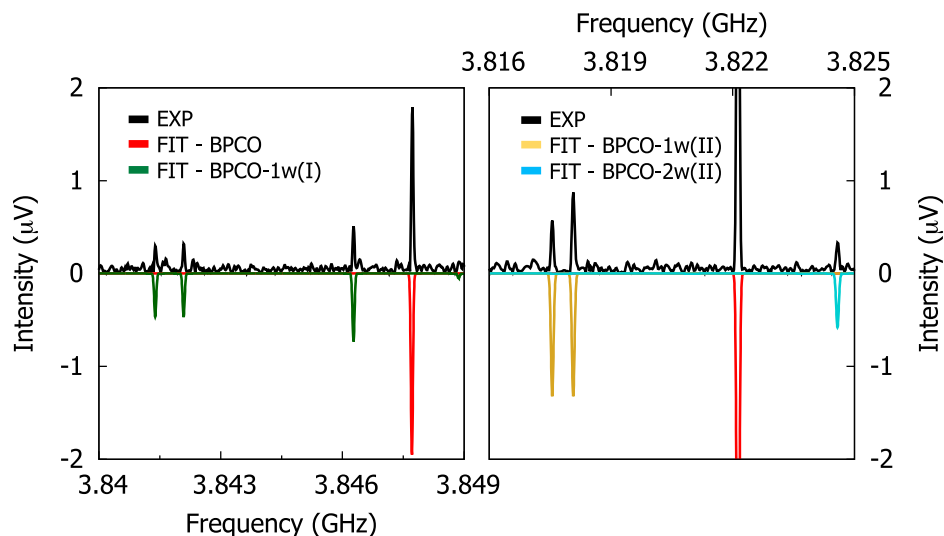^{b}6-311G++(d,p) basis set.

FIG. 3. Two sections of the broadband rotational spectrum measured by adding water to the jet (2 M averages, 18 h of measurement time). The upper trace (in black) shows the experimental spectrum using neon as a carrier gas. The lower traces represent simulations obtained from the fitted spectroscopic parameters reported in Table I.

BPCO-1w(I) and BPCO-1w(II) are the two lowest energy minima, respectively, with the differential zero-point corrected energy being $\Delta_{ZPE}(1w(II)) = 1.7$ kJ/mol. Both quantum-chemical methods employed predict very well the observed rotational constants for the four observed species (see Table I). We find that the B3LYP-D3 calculations predict the experimental rotational constants more accurately than the MP2 calculations, while the dipole-moment components are better reproduced by the MP2 calculations, in particular for 2w(II).

In order to further elucidate the structures of the molecular complexes, we performed an additional measurement where we seeded our jet with an isotopically enriched sample of water with *ca.* 50% $H_2^{18}O$ (2M averages, 18 h of measurement time). This allowed us to observe the rotational spectra of isotopically substituted BPCO-1w(I)(^{18}O), BPCO-1w(II)(^{18}O), and BPCO-2w(II)(^{18}O) and thus obtain experimentally the positions of the oxygens for the water molecules using the r_s method. An overlay of the predicted structures with the experimentally determined positions of the water oxygen atoms is shown in Fig. 4. The good agreement between experiment and theory secures our confidence in the structural assignment and provides further structural information. Spectroscopic parameters

for the isotopically substituted species are given in the supplementary material.

We find that a single water molecule can bind to BPCO via two different docking sites (see Fig. 4). The two geometries have a similar configuration since they encompass O–H···O hydrogen bonds between the water and the carbonyl group of BPCO. However, 1w(I) is additionally stabilised by a weak C–H···O secondary interaction with the adjacent phenyl ring. In the complex 1w(II), the water does not interact with the phenyl ring. These configurations are in agreement and consistent with the calculated energies that predict 1w(I) to be more stable than 1w(II), the additional interaction in 1w(I) likely being responsible for the additional stability of the complex. Furthermore, in 1w(I) the position of the water molecule is better defined compared with that of 1w(II). This result is consistent with the lack of a secondary interaction in 1w(II), preventing similar stabilities for both complexes. We also note that the different docking locations for the water molecule in the one-water clusters, 1w(I) and 1w(II), result in distinct spectral signatures, an a-type vs. a b-type spectrum, respectively.

Interestingly, we identify a single binding geometry for the two-water cluster, 2w(II). The two water molecules form a dimer that links both sides of BPCO resembling a water

BPCO-1w(I)

a / OH..O (1.973 Å)
O .. O (2.909 Å)
b / O .. H (2.351 Å)
O .. C (3.399 Å)
ϕ / -52.7º
(B3LYP-D3)

BPCO-1w(II)

a / OH..O (1.965 Å)
O .. O (2.858 Å)
ϕ / -51.8º
(B3LYP-D3)

BPCO-2w(II)

a / OH..O (1.888 Å)
O .. O (2.822 Å)
c / O .. H (2.443 Å)
O .. C (3.197 Å)

b / OH..O (1.875 Å)
O .. O (2.839 Å)
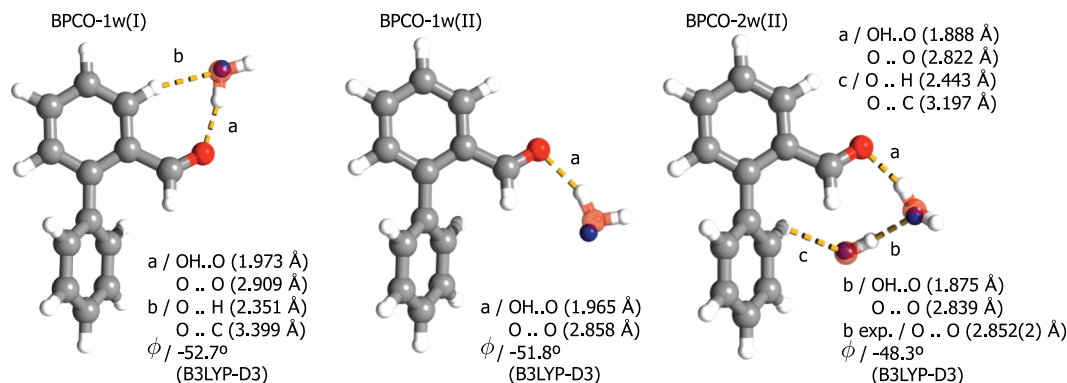b exp. / O .. O (2.852(2) Å)
ϕ / -48.3º
(B3LYP-D3)

FIG. 4. Calculated structures, dominant intermolecular interactions, and angles ϕ for the observed first- and second-order molecular clusters of BPCO and water. All depicted structures were obtained at the B3LYP-D3/aug-cc-pVTZ level of theory. The structures of the BPCO-water clusters are overlaid with the experimentally determined positions of the oxygen atoms of the water molecules (blue spheres).
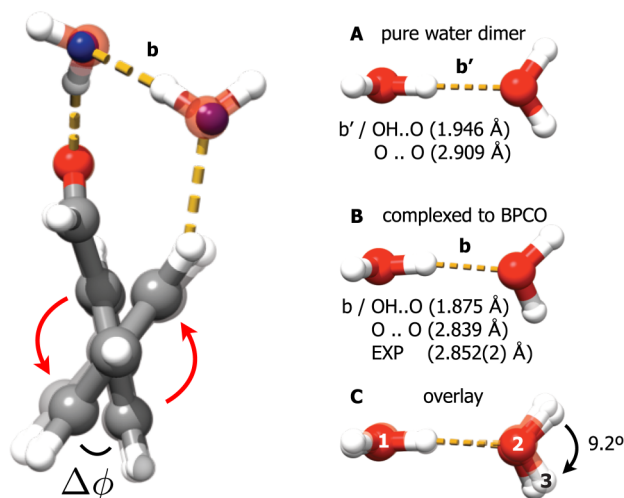
FIG. 5. Left: Overlay of free BPCO and BPCO-2w(II) calculated at the B3LYP-D3/aug-cc-pVTZ level of theory. The structure of free BPCO has been set to semi-transparent to highlight the different angles ϕ for the two systems. Right: (A) water dimer structure obtained at the same level of theory depicting relevant interatomic distances; (B) geometry of the water dimer complexed to BPCO, which is removed for clarity; (C) overlay of the two water dimer structures depicting the change in the orientation of hydrogens. The angle is determined by the numbered atoms 1, 2, and 3.

TABLE II. Energy decomposition (kJ/mol) obtained from a SAPT(0)/jun-cc-pVDZ calculation on all three observed water complexes with BPCO. ΔE_{elec} is the electrostatic energy; ΔE_{ind} is the induction energy accounting for charge transfer interactions; ΔE_{disp} is the energy contribution from dispersion interactions; ΔE_{exch} represents the repulsion due to exchange.

	ΔE_{elec}	ΔE_{ind}	ΔE_{disp}	ΔE_{exch}	ΔE_{tot}
1w(I)	−43.3	−11.2	−10.3	34.9	−30.0
1w(II)	−39.1	−10.4	−9.2	31.7	−27.1
2w(II)	−61.4	−19.1	−15.9	49.8	−46.8

wire. When comparing the angle ϕ, defined by the two planes containing each phenyl ring (see Figs. 1 and 5), for bare BPCO, BPCO-1w(I), BPCO-1w(II), and BPCO-2w(II), we observe an interesting trend towards decreasing ϕ (Table I and Fig. 4). By comparing the angle ϕ of the free and wired BPCO, we find that the addition of water reduces ϕ by approximately 5°, i.e., the binding interactions seem to partly cancel some of the steric hindrance. This change in ϕ for BPCO is consistently predicted by both *ab initio* and density functional theory calculations (see Table I). Moreover, we note that in the 2w(II) complex, the water molecule interacting with the carbonyl group adopts a binding geometry similar to that of 1w(II) and not as 1w(I).

The free BPCO is stabilised in a non-planar configuration due to steric hindrance additionally influenced by the carbonyl group. Electrostatic repulsion locks the system in this configuration where stereo-inversion is separated by an energy barrier of *ca.* 5 kJ/mol (420 cm^{-1}, see Fig. 1). Upon complexation, the water wire perturbs the initial electrostatic balance. Revealing the mechanisms for aggregation of the water wire to BPCO and providing a quantitative analysis of all the effects at play here are not trivial.[12,24]

As a first step in that direction, we performed zeroth-order symmetry adapted perturbation theory (SAPT)[25] calculations to decompose the energetic contributions arising from intermolecular binding forces in 1w(I), 1w(II), and 2w(II). SAPT(0)/jun-cc-pVDZ[26] calculations were performed using the B3LYP-D3 optimised structures as starting geometries. The jun-cc-pVDZ is a reduced form of the aug-cc-pVDZ basis set. The calculations were performed using the Psi4 electronic structure package[27] and the results are shown in Table II. There is a clear indication that hydrogen bonding is the dominant contribution for all three water-bound complexes. The ΔE_{elec} contribution arises mainly from O–H···O hydrogen

bonds as depicted in Fig. 4 (interaction marked as *a*). The energetic contributions for the 2w(II) complex were computed employing the water dimer as a single molecular unit. As such, the proportion of energetic contributions in 2w(II) compared with those of 1w(I) and 1w(II) are similar, which consistently agrees with the fact that in all three water complexes a single strong O–H···O interaction is present between water and the solute.

As a tentative model, we propose here a water binding mechanism through the interaction of an already formed water dimer and free BPCO. In Fig. 5 (left) we show an overlay of the observed conformations of free BPCO and BPCO linked via the water wire. The predicted change of 5° in the dihedral angle ϕ for the 2w(II) complex is depicted in the overlay of complexed and uncomplexed species. Furthermore, we show in Fig. 5 (right) a comparison of the free and complexed water dimer geometries. The experimentally determined O···O distance (2.852(2) Å) and relative orientation of the water molecules, with respect to each other, show that the dimer forming the 2w(II) complex undergoes a distortion. In addition to a measurable shortening of the O···O distance in the wire compared with that of the free water dimer (2.909 Å), the changing orientation (9.2°) indicates that the dimer adopts a geometry that facilitates the binding interaction with BPCO. We find that a delicate balance between conformational changes in BPCO, via a change of ϕ, and distortion of the water dimer, via shortening of O···O, results in a stable cluster. Relevant bond distances for the cluster are shown in Figs. 4 and 5.

To conclude, we used high-resolution rotational spectroscopy to determine experimentally the structure of an axially chiral molecule of the biphenyl family and of three different complexes with water. We find that the second-order water cluster forms a wire that connects the two phenyl moieties, which leads to a measurable change of the dihedral angle between the two phenyl moieties of the BPCO upon complexation. We investigated this effect considering hydrogen bonding interactions between water and the axially chiral molecule. As our results show, specific interactions between a small number of water molecules and a biochemical ligand result in conformational changes that may influence further interaction mechanisms. Explicit considerations of solvated sites within the target molecule, in particular for systems with axial symmetry, will provide a more complete description of the molecular system under investigation. This result, while addressing a particular type of chiral systems containing axial symmetry, carries general implications regarding water

interactions playing a mediating role in ligand-receptor interactions. Our observations may extend to other molecules with axial symmetry outside of the biphenyl family. Structural rearrangements from both ligand and water moieties may cooperate towards optimising further interactions with other more complex molecular systems, such as biological receptors.

See the supplementary material for further details of experimental methods, rotational constants of all reported species, Kraitchman calculations, and line lists with all fitted rotational transitions.

[1]Y. M. Rhee, E. J. Sorin, G. Jayachandran, E. Lindahl, and V. S. Pande, "Simulations of the role of water in the protein-folding mechanism," Proc. Natl. Acad. Sci. U. S. A. **101**, 6456–6461 (2004).

[2]J. F. Nagle and H. J. Morowitz, "Molecular mechanisms for proton transport in membranes," Proc. Natl. Acad. Sci. U. S. A. **75**, 298–302 (1978).

[3]H. Wang and A. Ben-Naim, "A possible involvement of solvent-induced interactions in drug design," J. Med. Chem. **39**, 1531–1539 (1996).

[4]B. M. Giuliano and W. Caminati, "Isotopomeric conformational change in anisolewater," Angew. Chem. Int. Ed. **44**, 603–606 (2005).

[5]A. Gutberlet, G. Schwaab, O. Birer, M. Masia, A. Kaczmarek, H. Forbert, M. Havenith, and D. Marx, "Aggregation-induced dissociation of hcl(h2o)4 below 1k: The smallest droplet of acid," Science **324**, 1545–1548 (2009).

[6]W. Caminati, J. C. López, S. Blanco, S. Mata, and J. L. Alonso, "How water links to *cis* and *trans* peptidic groups: The rotational spectrum of *N*-methylformamide-water," Phys. Chem. Chem. Phys. **12**, 10230–10234 (2010).

[7]L. Evangelisti and W. Caminati, "Internal dynamics in complexes of water with organic molecules. Details of the internal motions in tert-butylalcohol-water," Phys. Chem. Chem. Phys. **12**, 14433–14441 (2010).

[8]H. Fricke, K. Schwing, A. Gerlach, C. Unterberg, and M. Gerhards, "Investigations of the water clusters of the protected amino acid ac-phe-ome by applying ir/uv double resonance spectroscopy: Microsolvation of the backbone," Phys. Chem. Chem. Phys. **12**, 35113521 (2010).

[9]H. Zhu, M. Blom, I. Compagnon, A. M. Rijs, S. Roy, G. von Helden, and B. Schmidt, "Conformations and vibrational spectra of a model tripeptide: Change of secondary structure upon micro-solvation," Phys. Chem. Chem. Phys. **12**, 3415–3425 (2010).

[10]J. Thomas, O. Sukhorukov, W. Jäger, and Y. Xu, "Direct spectroscopic detection of the orientation of free oh groups in methyl lactate(water)1,2 clusters: Hydration of a chiral hydroxy ester," Angew. Chem. Int. Ed. **53**, 1156–1159 (2014).

[11]D. P. Tabor, R. Kusaka, P. S. Walsh, E. L. Sibert III, and T. S. Zwier, "Isomer-specific spectroscopy of benzene(h2o)n, n = 6,7: Benzenes role in reshaping waters three-dimensional networks," J. Phys. Chem. Lett. **6**, 1989–1995 (2015).

[12]C. Pérez, A. Krin, A. L. Steber, J. C. López, Z. Kisiel, and M. Schnell, "Wetting camphor: Multi-isotopic substitution identifies the complementary roles of hydrogen bonding and dispersive forces," J. Phys. Chem. Lett. **7**, 154–160 (2016).

[13]S. Blanco, P. Pinacho, and J. C. López, "Hydrogen-bond cooperativity in formamide2-water: A model for water-mediated interactions," Angew. Chem. Int. Ed. **128**, 9477–9481 (2016).

[14]*Handbook of High-resolution Spectroscopy*, edited by M. Quack and F. Merkt (John Wiley & Sons, Ltd., 2011).

[15]G. G. Brown, B. C. Dian, K. O. Douglass, S. M. Geyer, S. T. Shipman, and B. H. Pate, "A broadband Fourier transform microwave spectrometer based on chirped pulse excitation," Rev. Sci. Instrum. **79**, 053103 (2008).

[16]D. Schmitz, V. A. Shubert, T. Betz, and M. Schnell, "Multi-resonance effects within a single chirp in broadband rotational spectroscopy: The rapid adiabatic passage regime for benzonitrile," J. Mol. Spectrosc. **280**, 77–84 (2012).

[17]C. Pérez, S. Lobsiger, N. A. Seifert, D. P. Zaleski, B. Temelso, G. C. Shields, Z. Kisiel, and B. H. Pate, "Broadband Fourier transform rotational spectroscopy for structure determination: The water heptamer," Chem. Phys. Lett. **571**, 1–15 (2013).

[18]S. R. Domingos, C. Pérez, C. Medcraft, P. Pinacho, and M. Schnell, "Flexibility unleashed in acyclic monoterpenes: Conformational space of citronellal revealed by broadband rotational spectroscopy," Phys. Chem. Chem. Phys. **18**, 16682–16689 (2016).

[19]M. J. Frisch, G. W. Trucks, H. B. Schlegel, H. B. Scuseria, M. A. Robb, J. R. Cheeseman, G. Scalmani, V. Barone, B. Mennucci, G. A. Petersson, H. Nakatsuji, M. Caricato, X. Li, H. P. Hratchian, A. F. Izmaylov, J. Bloino, G. Zheng, J. L. Sonnenberg, M. Hada, M. Ehara, K. Toyota, R. Fukuda, J. Hasegawa, M. Ishida, T. Nakajima, Y. Honda, O. Kitao, H. Nakai, T. Vreven, J. A. Montgomery, Jr., J. E. Peralta, F. Ogliaro, M. Bearpark, J. J. Heyd, E. Brothers, K. N. Kudin, V. N. Staroverov, R. Kobayashi, J. Normand, K. Raghavachari, A. Rendell, J. C. Burant, S. S. Iyengar, J. Tomasi, M. Cossi, N. Rega, J. M. Millam, M. Klene, J. E. Knox, J. B. Cross, V. Bakken, C. Adamo, J. Jaramillo, R. Gomperts, R. E. Stratmann, O. Yazyev, A. J. Austin, R. Cammi, C. J. Pomelli, W. Ochterski, R. L. Martin, K. Morokuma, V. G. Zakrzewski, G. A. Voth, P. Salvador, J. J. Dannenberg, S. Dapprich, A. D. Daniels, O. Farkas, J. B. Foresman, J. V. Ortiz, J. Cioslowski, and D. J. Fox, GAUSSIAN 09, Revision C.02, Gaussian, Inc., Wallingford, CT, 2009.

[20]J. Zhang and M. Dolg, "Abcluster: The artificial bee colony algorithm for cluster global optimization," Phys. Chem. Chem. Phys. **17**, 24173–24181 (2015).

[21]C. M. Western, "PGOPHER: A program for simulating rotational, vibrational and electronic spectra," J. Quant. Spectrosc. Radiat. Transfer (in press).

[22]J. Kraitchman, "Determination of molecular structure from microwave spectroscopic data," Am. J. Phys. **21**, 17–24 (1953).

[23]Z. Kisiel, "Assignment and analysis of complex rotational spectra," in *Spectroscopy from Space*, edited by J. Demaison *et al.* (Kluwer Academic Publishers, 2001), pp. 91–106.

[24]C. Pérez, J. L. Neill, M. T. Muckle, D. P. Zaleski, I. Peña, J. C. López, J. L. Alonso, and B. H. Pate, "Water-water and water-solute interactions in microsolvated organic complexes," Angew. Chem. Int. Ed. **54**, 979–982 (2015).

[25]B. Jeziorski, R. Moszynski, and K. Szalewicz, "Perturbation theory approach to intermolecular potential energy surfaces of van der Waals complexes," Chem. Rev. **94**, 1887–1930 (1994).

[26]T. M. Parker, L. A. Burns, R. M. Parrish, A. G. Ryno, and C. D. Sherrill, "Levels of symmetry adapted perturbation theory (sapt). I. efficiency and performance for interaction energies," J. Chem. Phys. **140**, 094106 (2014).

[27]J. M. Turney, A. C. Simmonett, R. M. Parrish, E. G. Hohenstein, F. A. Evangelista, J. T. Fermann, B. J. Mintz, L. A. Burns, J. J. Wilke, and M. L. Abrams, "Psi4: An open-source *ab initio* electronic structure program," Wiley Interdiscip. Rev.: Comput. Mol. Sci. **2**, 556–565 (2012).